

## Effect of print parameters on the tensile strength and built time of FDM-printed PLA parts

This Accepted Manuscript (AM) is a PDF file of the manuscript accepted for publication after peer review, when applicable, but does not reflect post-acceptance improvements, or any corrections. Use of this AM is subject to the publisher's embargo period and AM terms of use. Under no circumstances may this AM be shared or distributed under a Creative Commons or other form of open access license, nor may it be reformatted or enhanced, whether by the Author or third parties. By using this AM (for example, by accessing or downloading) you agree to abide by Springer Nature's terms of use for AM versions of subscription articles: <https://www.springernature.com/gp/open-research/policies/accepted-manuscript-terms>

The Version of Record (VOR) of this article, as published and maintained by the publisher, is available online at: <https://doi.org/10.1007/s00170-024-13506-x>. The VOR is the version of the article after copy-editing and typesetting, and connected to open research data, open protocols, and open code where available. Any supplementary information can be found on the journal website, connected to the VOR.

For research integrity purposes it is best practice to cite the published Version of Record (VOR), where available (for example, see ICMJE's guidelines on overlapping publications). Where users do not have access to the VOR, any citation must clearly indicate that the reference is to an Accepted Manuscript (AM) version.

## Effect of print parameters on the tensile strength and built time of FDM-printed PLA parts

Asif Hasan<sup>1,\*</sup>, Muhammad Fahad<sup>2</sup>, Maqsood Ahmed Khan<sup>1</sup>

<sup>1</sup>Department of Industrial & Manufacturing Engineering, NED University of Engineering and Technology, Karachi, Pakistan

<sup>2</sup>School of Digital Technologies and Arts, Staffordshire University, Stoke-on-Trent, Staffordshire, England

\*Corresponding author email: [asif.hasan@hotmail.com](mailto:asif.hasan@hotmail.com)

Email: Muhammad Fahad, [muhhammad.fahad@staffs.ac.uk](mailto:muhhammad.fahad@staffs.ac.uk); Maqsood Ahmed Khan, [maqsoodahmed@neduet.edu.pk](mailto:maqsoodahmed@neduet.edu.pk)

Accepted manuscript

**Abstract**

Commented [LS1]: CE: Please capture the rights retention information correctly.

Fused Deposition Modeling (FDM) is an additive manufacturing (AM) technique based on the principle of forced extrusion. It is the most commonly used 3D printing processes, subjected to its ease of utilization. With the increase in product customizations, the use of 3D printing technique for manufacturing of the end-use product is on the rise. Therefore, the strength and other mechanical properties of the 3D-printed finished component are of great importance. These mechanical properties of an FDM-produced part are greatly affected by the selection of different values for printing parameters. Due to operational simplicity and low cost, FDM is widely researched, and a number of scholars have examined the effects of varying the values of parameters on the mechanical properties of the FDM-printed specimens. Where tensile strength of the 3D-printed parts is the mostly studied property among all mechanical properties. However, the effect of changing values of parameters on the tensile strength in relation to build time is least researched. The objective of this research is not only to examine the influence of printing parameters such as layer thickness, print angle, and infill density on the tensile strength of the 3D-printed components and optimize them but also to achieve the desired strength in a faster and timely manner. In this study, tensile test specimens were printed and tested according to ISO-527-2 standards. Analysis of variance (ANOVA) is also performed to check the significance of print parameters. The results suggested that an increase in layer thickness has an inverse impact on the tensile strength, whereas an increase in print angle and infill density has a direct impact on the tensile properties of the FDM produced specimens. Furthermore, the print time is reduced with an increase in layer thickness and a decrease in infill density, as both lead to fewer passes required to print the part. However, print time has variable relationship with the print angle, with the least value at a 90° print angle and the maximum value at a 15° print angle.

**Keywords:** 3D printing, Fused Deposition Modeling, Tensile strength, Process parameters, Built time, ANOVA

## 1. Introduction

Additive manufacturing (AM) is a process in which a three-dimensional object is developed by adding layers of material over previous layer with a computer controlled procedure. There are 07 (seven) different categories of AM technology [1, 2]. Among these categories, Fused Deposition Modeling (FDM) process in Material Extrusion category stands out as the most extensively used additive manufacturing process for fabricating prototypes and general engineering parts for end-use [3]. Fused Deposition Modeling (FDM), also known as Fused Filament Fabrication (FFF), operates as an extrusion-based process, in which semi-liquefied material is forced out of a orifice or outlet [2].

The production of parts using additive manufacturing techniques does not require any specialized tooling, and complex geometries can be produced very easily using these AM techniques. Moreover, several sub-assemblies can be produce as a single component with the help of AM techniques [4]. With the rapid growth in the use of AM technology, this technique is not only used to evaluate fit, form, ergonomics and functionality of the prototypes [5], but in fact, it is also use to produce customized products at comparatively lower cost than conventional methods [6].

It is a general observation that FDM-printed parts exhibit weaker mechanical properties when compared to conventionally produce counter parts since they exhibit anisotropic behavior. This might limit the scope of 3D-printed parts. However, the emergence of technology has broadened its domain of application in fields of prosthetics, medicine, electronics, automotive, and aerospace and in general for mechanical replacement of the parts [7].

As the AM technique is now being used for end-use custom parts, the mechanical strength of components produced using 3D printing techniques is of great interest. The FDM technique includes several print parameters that, when varied, significantly alter the mechanical behavior of the printed parts. Furthermore, variations in these print parameters also affect the printing time and the associated material cost.

Scholars and researchers have extensively studied the mechanical strength of 3D-printed parts using the FDM technique as a result of varying printing parameters. The most commonly varied parameters for the FDM process include the following [8, 9]:

1. Infill pattern: The internal configuration of the beads inside the core volume of a part in a single layer.
2. Layer thickness: The height of every subsequent stratum.
3. Print angle or raster angle: Is the direction in which beads are laid relative to the loading or part for functional test [10] or the direction of the bead in reference to  $x$ -axis of building platform.
4. Infill density: The volume of substance contained within the geometry.
5. Build orientation: The direction of the object's geometry in which it is built inside the building chamber.
6. Print speed: The speed at which the part is printed at built platform. It is also referred as the traveling speed of the printing head.
7. Raster width (also known as bead width): The side-wise thickness of a bead in a layer.
8. Air gap: Space between two neighboring beads.
9. Extrusion temperature: Temperature of the nozzle during printing.
10. No. of perimeter shell: Shell is the outer wall or the final shape of the part. No. of shells defines the thickness of the outer wall.

Different types of materials are used to fabricate FDM parts that sufficiently qualify for prototyping, functional testing, and, most importantly, custom-made end-use products. However, Poly Lactic Acid (PLA) and Acrylonitrile Butadiene Styrene (ABS) are the most frequently used and studied materials [10]. Due to its better stability against shrinkage, moisture absorption, warpage, improved industrial feasibility, and biodegradability [11], Poly Lactic Acid (PLA) is selected for this study and will be discussed further.

Poly Lactic Acid (PLA) is a biodegradable and bioactive thermoplastic aliphatic polyester derived from renewable (plant-based) resources such as cassava roots, corn starch, or sugarcane. Therefore, it is also called "the green plastic." It has a density of  $1.25 \text{ gm/cm}^3$ , a melting point around  $200^\circ\text{C}$ , and is insoluble in water [12]. The use of PLA expanded into the packaging and biomedical industries ever since a commercialized production line was established in 2003 [13]. PLA has become ubiquitous in the field of bio-medics due to its attractive peculiarities, including

biocompatibility, hydrolytic degradation, and tailorable properties. This has led to the development of several PLA applications, such as bone fixation screws, special-purpose suture threads, and stent coatings [14].

The impact of FDM process parameters on the mechanical strength of the PLA parts has been extensively studied by several researchers over the last decade. Among the earliest studies, one was performed by Tymrak [15] using PLA material. They studied the effects of layer thickness and raster angle on modulus of elasticity and tensile strength. Since then, many scholars have researched the influence of printing parameters on properties of the FDM printed parts. Most of these studies focus on evaluating the tensile strength of the printed components [16–19], with the major emphasis on optimizing the printing parameters for better results [20–22]. Some researchers have also explored other mechanical properties, such as modulus of elasticity [15, 23, 24], strain at break [25], compressive strength [26, 27], impact strength [26, 28, 29], and flexural strength [29–31]. This study will primarily concentrate on three key printing parameters: layer thickness, print angle, and infill density. These parameters have been thoroughly investigated by other researchers and are acknowledged as significant factors influencing the mechanical strength of printed parts. It is anticipated that they also play a crucial role in optimizing print time. Moreover, choosing a higher number of parameters not only extends the time required for evaluation but may also introduce interactions that could impact the main effects of other parameters.

Layer thickness is the most researched parameter of all and is found to have substantial effect on the tensile properties of the printed part. Tymrak [15] and Lanzotti [25] evaluated that layer thickness has a variable relationship with tensile strength. They found that an increase in layer thickness initially decreases and then increases the tensile strength, reaching maximum strength at minimum layer thickness. However, Li et al. [19], Li et al. [20], Rodríguez-Panes et al. [24], and Liu et al. [29] observed an inversely proportional relationship between layer thickness and tensile strength—higher layer thickness resulted in reduced tensile strength. On the other hand, some researchers [32–35] concluded that the increase in layer thickness enhances the tensile strength.

Raster angle or “print angle” is the second most commonly studied printing parameter. It has been researched in two different variations: crisscross rasters and unidirectional rasters. For

unidirectional rasters, a few researchers [18, 21, 25] concluded that the maximum tensile strength is observed when the direction of rasters is parallel to the applied force. As the direction of the rasters changes from parallel towards perpendicular to the applied force, the tensile strength of the part decreases. Song et al. [26] studied three different values of raster angle ( $0^\circ$ ,  $45^\circ$ , and  $90^\circ$ ) and found the maximum strength at  $45^\circ$  rasters. Torres et al. [32], studying two crisscross variations ( $0^\circ/90^\circ$  and  $45^\circ/135^\circ$ ), found that the effect of raster angle is insignificant for tensile strength. However, Tymrak [15], Rajpurohit [18], and Tao [34] studied multiple crisscross arrangements of rasters and found maximum strength at different criss-cross combinations. The findings from various studies indicate that layer thickness and print angle play a crucial role in determining the tensile strength of 3D-printed parts. However, there is no consensus on the nature of its impact, leaving it unclear whether layer thickness has a direct, inverse, or different kind of effect on tensile strength. Consequently, there is a pressing need to carry out experiments aimed at examining how variations in layer height and print angle will affect the tensile strength of printed part.

Nevertheless, studies [16, 19, 24, 32, 33] investigating the link between the tensile strength of a part and its infill density have consistently found comparable outcomes. The findings indicate that an increase in infill density enhances the mechanical strength of the printed parts. This improvement is attributed to the fact that a higher density leads to the material being more tightly packed within the component. This compact arrangement of material contributes to making the part stronger by enhancing its ability to withstand tension.

Within all these research studies, the main focus of the researchers is to identify the key influential parameters that have a major effect on the mechanical properties of the printed part. However, a limited number of researchers have delved into the examination of build time concerning the desired mechanical strength of 3D-printed components [36-38]. Le et al. [36] explored five parameters (number of perimeter shells, nozzle diameter, extrusion temperature, infill pattern, and infill percentage) with the goal of optimizing print time for maximum strength. Bintara et al. [37] investigated the impact of layer height on surface roughness, considering its relationship with print time. Maurya et al. [38] concentrated on the influence of infill pattern and infill density on the printing time and dimensional accuracy of 3D-printed cubes.

Taking into account the findings from prior research, this study aims to examine how certain chosen parameters influence the tensile strength of components printed using Fused Deposition Modeling (FDM), as well as the duration needed to print these components. The goal is to enhance the tensile strength of the printed parts while also optimizing the printing time. To identify the statistical importance of these selected parameters, an ANOVA (Analysis of Variance) analysis will be conducted. Furthermore, a regression model will be developed to predict the tensile strength and corresponding printing time for a specific set of parameters. This approach allows for a comprehensive understanding of how adjustments in printing settings can affect both the mechanical properties and the efficiency of the FDM printing process.

## 2. Materials and methods

### 2.1. 3D printer and material

In this research, FDM tensile test specimens were printed using PLA (Poly Lactic Acid) material provided by eSun Industrial Co. Ltd. (Shenzhen, China). The properties of the PLA filament used to print the components are presented in Table 1.

**Table 1** Properties of PLA material (as provided by the manufacturer)

S #	Properties	Values
1	Print temperature °C	190–220
2	Bed temperature °C	60–80
3	Density (gm/cm <sup>3</sup> )	1.25
4	Heat distortion temperature	56 (at 0.45 MPa)
5	Melt flow index (gm/10 min)	5 (190°C/2.16 kg)
6	Flexural modulus (MPa)	3600
7	Elongation at break (%)	8

8	Tensile strength (MPa)	65
9	IZOD impact strength (kJ/m <sup>2</sup> )	4
10	Flexural strength (MPa)	97
11	Filament diameter (mm)	1.75

Tensile test specimens were printed using Creality Ender-3 Pro (Creality 3D, Shenzhen, China) printer. This printer has only one printing nozzle; therefore, only one (single) type of material can be used to print both parts and support structure. Table 2 shows the main characteristics of the printer as provided by the manufacturer.

**Table 2** Main characteristics of printer

S #	Properties	Values
1	Build volume (mm <sup>3</sup> ) [ <i>X</i> × <i>Y</i> × <i>Z</i> ]	220 × 220 × 250
2	Nozzle diameter (mm)	0.4 (can be changed to 0.2 & 0.3)
3	Filament diameter (mm)	1.75
4	<i>XY</i> accuracy (mm)	0.1
5	<i>Z</i> resolution (mm)	0.1
6	No. of print head(s)/extruder(s)	1

Printing parameters such as raster angle, layer thickness, and print speed are varied using Ultimate Cura (version 4.12) slicing software.

## 2.2. Experimental design

In order to comprehend the influence of printing parameters on the mechanical properties of tensile test specimens, three process parameters were investigated, each with their respective variations as mentioned in Table 3. The layer thickness was varied from 0.1 mm to 0.3 mm in 0.1 mm increments. Print angle is varied from 0° to 90° such that at 0° all rasters in the infill are perpendicular to the direction of the applied force, whereas at a print angle of 90°, all rasters in the infill are parallel to the direction of the applied force, as shown in Fig. 2. And Infill density is varied between 50% and 100% in 25% increments. The chosen values for the selected parameters are based on a thorough literature review, as they represent commonly tested values by numerous researchers in previous studies. Selecting these values allows for meaningful comparisons with the results obtained in prior research, providing a basis for evaluating and contextualizing the outcomes of our study. To maintain consistent print quality across all samples, all other process parameters were kept constant at the values specified in Table 4.

**Table 3** Variable printing parameters along with their variations

S #	Printing parameters	Variations
1	Layer thickness (mm)	0.1, 0.2, & 0.3
2	Infill density (%)	50, 75, & 100
3	Print angles (Deg)	0, 15, 30, 45, 60, 75, & 90

**Table 4** Fixed printing parameters in this study

S #	Fixed printing parameters	Value
1	Print speeds (mm/min)	60

2	Bed temperature (°C)	60
3	Extrusion temperature (°C)	200
4	Infill pattern	Line
5	Part built orientation	Flat
6	No. of shell perimeters	4

**Fig. 1** Print angle in the infill of specimens, no. of perimeter shells, and direction of applied force (F)

A full factorial design for the aforementioned parameters resulted in 63 types of sample, as mentioned in Table 5. Repeatability of outcomes was ensured by producing five replicates for each sample type, and therefore, a sum of 315 samples was printed for tensile testing. FDM tensile test specimens used during this study were designed as per ISO 527-2-2012 [39] (International standard to determine the tensile strength of plastic specimens). The measurements of sample are presented in Fig. 1. The technical soft model of sample was generated using Creo-Parametric 3 and slicing software used was Cura Ultimaker (Version 4.12).

**Fig. 2** ISO 527-2 sample shape and size (All dimensions are in MM) [39]

**Table 5** Total experimental runs across all combinations of process parameters

Experiment #	Print angles (Deg)	Layer thickness (mm)	Infill density (%)
1/22/43	0	0.1	100/75/50
2/23/44	15	0.1	100/75/50
3/24/45	30	0.1	100/75/50
4/25/46	45	0.1	100/75/50
5/26/47	60	0.1	100/75/50
6/27/48	75	0.1	100/75/50
7/28/49	90	0.1	100/75/50
8/29/50	0	0.2	100/75/50
9/30/51	15	0.2	100/75/50
10/31/52	30	0.2	100/75/50
11/32/53	45	0.2	100/75/50
12/33/54	60	0.2	100/75/50
13/34/55	75	0.2	100/75/50
14/35/56	90	0.2	100/75/50
15/36/57	0	0.3	100/75/50
16/37/58	15	0.3	100/75/50
17/38/59	30	0.3	100/75/50
18/39/60	45	0.3	100/75/50
19/40/61	60	0.3	100/75/50
20/41/62	75	0.3	100/75/50
21/42/63	90	0.3	100/75/50

Table 5 outlines every possible combination of settings used in the experimental runs. The table is organized in a concise format for easier understanding. To interpret the table, for instance, Experiment #1 is set up with a print angle of 0°, a layer thickness of 0.1mm, and an infill density of 100%. On the other hand, Experiment #22 is configured with the same print angle of 0° and layer thickness of 0.1mm, but with a reduced infill density of 75%. Similarly, Experiment #43 is detailed to have a print angle of 0°, a layer thickness of 0.1mm, and an infill density of 50%. This systematic arrangement allows for a clear representation of the varying experimental conditions across different runs.

### 2.3. Tensile testing

Quasi static tensile test were carried out to study the tensile strength and elongation of PLA specimens. The Universal Testing Machine (UTM) used for testing was from LLOYD Instruments, Model LR10K Plus with maximum load capacity of 10 KN. The strain rate as per standard is 5 mm/min but to increase energy absorbed before failure, strain rate was deliberately kept at 1 mm/min as per previous research [8], and the temperature was maintained at 23°C. Extensometers were used to measure the elongation/strain in the specimens. All the above equipment is shown in Fig. 3.

**Fig. 3** Uniaxial tensile test

### 3. Results

#### 3.1. Analysis for tensile strength

Results of tensile strength (MPa) of all the samples are presented in Table 6. These results are the mean value of the five samples for each set of parameters. The variation in tensile strength (MPa) pertaining to layer thickness (mm) at different print angles (Deg) for all levels of infill density (100%, 75%, and 50%) is presented in Fig. 4. The greatest value for tensile strength (50.39 MPa) was achieved at 0.1-mm layer thickness, 90° raster angle, and 100% infill density while the smallest value of tensile strength (8.25 MPa) was found at 0.3-mm layer thickness, 0° raster angle, and 50% infill density. Therefore, this can be concluded that for higher tensile strength, material in a specimen is needed to closely pack inside the volume of the geometry, although it will require more time to print a dense part.

**Table 6** Average tensile strength (MPa) of the specimens

		Mean tensile strength (MPa)								
		Infill density 100%			Infill density 75%			Infill density 50%		
		Layer thickness (MM)			Layer thickness (MM)			Layer thickness (MM)		
		0.1	0.2	0.3	0.1	0.2	0.3	0.1	0.2	0.3
Print angle (DEG)	0	32.94	31.18	28.85	15.66	14.63	13.68	9.16	8.73	8.25
	15	33.29	31.79	29.45	17.09	15.76	14.31	9.73	8.57	8.43
	30	35.07	33.21	30.44	17.44	15.99	15.39	10.39	9.93	9.17
	45	38.28	36.28	33.83	19.94	17.27	16.70	11.63	10.58	9.86
	60	43.65	42.02	39.81	21.33	20.17	18.81	13.83	12.58	12.14
	75	49.17	47.37	44.56	27.21	26.44	25.35	16.45	15.82	14.65
	90	50.39	48.51	44.86	40.29	39.01	36.55	34.16	32.62	29.57

**Fig. 4** Mean tensile strength (MPa) at different values of infill densities for constant value of layer thickness at different raster angles

Statistical tests were conducted to evaluate the importance of each selected parameter (print angle, layer thickness, and infill density) on both tensile strength and printing time. The outcomes of a nested ANOVA, focusing on the relationship between tensile strength versus the three selected print parameters, are detailed in Table 7, while the corresponding interval plots are illustrated in Fig. 5. The variance analysis demonstrates that the infill density and the print angle are significant determinants of the tensile strength in the printed object, while the layer thickness does not have a substantial impact. The analysis specifies that infill density has the highest influence, accounting for 73.14% of the variations in tensile strength, followed by the print angle with a 26.81% contribution. The interval plots further show a significant reduction in tensile strength as the infill density decreases from 100 to 75% and then to 50%. Similarly, tensile strength diminishes as the print angle moves from 90° (in line with the force applied) to 0° (perpendicular to the force applied). Though an increase in layer thickness from 0.1 mm to 0.3 mm also leads to a minor decrease in tensile strength, this change is considered statistically insignificant according to the ANOVA results.

**Table 7** Nested ANOVA: tensile strength (MPa) vs print angle (Deg), layer thickness (mm), and infill density (%)

Source	DF	SS	MS	F	P	Var. Comp.	% contribution	St Dev
Print angle (Deg)	6	16169.895	2694.9825	75.749	0.0	59.098	26.81	7.688
Layer thickness (mm)	14	498.0922	35.5780	0.044	1.0	-51.369*	0	0.000
Infill density (%)	42	33856.9413	806.1176	8126.156	0.0	161.204	73.14	12.697
Error	252	24.9985	0.0992			0.099	0.05	0.315
Total	314	50549.9269				220.401		14.846

\*Value is negative and is estimated by zero.

**Fig. 5** Interval plot for tensile strength (MPa) **a** for print angle [deg], **b** for infill density [%], and **c** for layer thickness [mm]

The influence of parameter interactions on tensile strength was assessed using two-way ANOVA, with findings for the interactions between print angle and layer thickness, print angle and infill density, as well as layer thickness and infill density, documented in Tables 8, 9, and 10, respectively. Figure 6 displays the corresponding interaction plot.

For the interaction between print angle and layer thickness (Table 8), the analysis indicated that print angle significantly affects tensile strength, but layer thickness and its interaction with print angle do not. The interaction plot shows that tensile strength tends to decrease as layer thickness increases across all print angles, though this decrease is deemed insignificant by ANOVA analysis. The highest strength was consistently found at a 90° print angle across all layer thicknesses, and the lowest is observed at 0° and 15° print angles.

The analysis of the interaction between print angle and infill density (Table 9) demonstrates that print angle, infill density, and their interaction all significantly impact tensile strength. The interaction plot for these variables shows a reduction in tensile strength with decreasing infill

density across all print angles. Notably, the decline in strength is more pronounced for angles below 90° at lower infill densities.

Finally, the interaction between layer thickness and infill density (Table 10) was found to have an insignificant effect on tensile strength. However, the interaction plot reveals that tensile strength significantly decreases with reduced infill density across all layer thicknesses, indicating that while their interaction may not be significant, infill density itself is a crucial factor for tensile strength.

**Table 8** Two-way ANOVA: tensile strength (MPa) vs print angle (Deg)-layer thickness (mm) interaction

Source	DF	SS	MS	F	P
Print angle (Deg)	6	16169.9	2694.98	23.38	0.0
Layer thickness (mm)	2	465.1	232.54	2.02	0.135
Interaction	12	33.0	2.75	0.02	1.0
Error	294	33881.9	115.24		
Total	314	50549.9			

$S = 10.74$ ,  $R^2 = 32.97\%$ , and  $R^2(\text{adj}) = 28.41\%$

**Table 9** Two-way ANOVA: tensile strength (MPa) vs print angle (Deg)-infill density (%) interaction

Source	DF	SS	MS	F	P
Print angle (Deg)	6	16169.9	2695.0	1322.78	0.0
Infill density (%)	2	32442.7	16221.4	7961.96	0.0
Interaction	12	1338.3	111.5	54.74	0.0

<b>Error</b>	294	599.0	2.0
<b>Total</b>	314	50549.9	

$S = 1.427$ ,  $R^2 = 98.82\%$ , and  $R^2 (\text{adj}) = 98.73\%$

**Table 10** Two-way ANOVA: tensile strength (MPa) vs print angle (Deg)-layer thickness (mm)  
Interaction

Source	DF	SS	MS	F	P
<b>Layer thickness (mm)</b>	2	465.1	232.5	4.05	0.018
<b>Infill density (%)</b>	2	32442.7	16221.4	282.37	0.0
<b>Interaction</b>	4	63.4	15.8	0.28	0.894
<b>Error</b>	306	17578.7	57.4		
<b>Total</b>	314	50549.9			

$S = 7.579$ ,  $R^2 = 65.22\%$ , and  $R^2 (\text{adj}) = 64.32\%$

**Fig. 6** Interaction plot for tensile strength (MPa)

### 3.2. Analysis for print time

The values for built time (mins) for all specimens were also recorded and are presented in Table 11. Comparison in built-time (mins) with respect to layer thickness (mm) at all values of raster angle (Deg) for all levels of infill density (%) is presented in Fig. 7.

**Table 11** Average built time (MINs) of the specimens

		Mean built time (MINs)								
		Infill density 100%			Infill density 75%			Infill density 50%		
		Layer thickness (MM)			Layer thickness (MM)			Layer thickness (MM)		
		0.1	0.2	0.3	0.1	0.2	0.3	0.1	0.2	0.3
Print angle (DEG)	0	105	55	40	93	48	35	77	41	30
	15	108	56	41	94	49	36	78	41	30
	30	104	54	39	91	48	35	79	41	30
	45	101	53	38	89	47	34	75	40	29
	60	97	51	37	87	46	33	86	45	33
	75	104	54	39	94	49	36	80	42	31
	90	93	48	35	82	43	31	70	37	27

**Fig. 7** Build-time (mins) at different values of infill densities for constant value of layer thickness at different raster angles

The results from a nested ANOVA, which investigates the correlation between print time and three selected printing parameters, are presented in Table 12. Additionally, Fig. 8 showcases the interval plots for this analysis. This variance analysis finds that layer thickness and infill density significantly influence the time it takes to print an object, whereas the print angle has no effect. Specifically, layer thickness is identified as the most impactful factor, responsible for 92.09% of the variation in print time, with infill density following at a 7.73% contribution. The main effect plot also indicates that print time significantly decreases as layer thickness increases from 0.1mm to 0.3mm. Similarly, a reduction in infill density from 100% to 50% leads to shorter print times. Changes in print angle, ranging from 0 to 90°, do not significantly affect print time, even though the shortest print time was observed at a 90° angle. Consequently, the ANOVA results deem the print angle to be statistically insignificant in influencing print time.

**Table 12** Nested ANOVA: print time (min) vs print angle (Deg), layer thickness (mm), and infill density (%)

Source	DF	SS	MS	F	P	Var. Comp.	% contribution	St Dev
Print angle (Deg)	6	1723.1746	287.1958	0.023	1.0	-276.879*	0	0
Layer thickness (mm)	14	178454.4444	12746.7460	36.577	0.0	826.550	92.09	28.750
Infill density (%)	42	14636.6667	348.4921	214.457	0.0	69.373	7.73	8.329
Error	252	409.5000	1.6250			1.625	0.18	1.275
Total	314	195223.7857				897.549		29.959

\*Value is negative and is estimated by zero.

**Fig. 8** Interval plot for print time [min] **a** for print angle [Deg], **b** for layer thickness [mm], and **c** for infill density [%]

The impact of different printing parameters on the duration required for printing was analyzed through a statistical method called two-way ANOVA. This analysis focused on how the combination of print angle and layer thickness, print angle and infill density, and layer thickness and infill density influence the overall print time. The outcomes of these interactions are detailed in Tables 13, 14, and 15, respectively, and an interaction plot illustrating these effects is shown in Figure 9.

Regarding the interaction between print angle and layer thickness (as shown in Table 13), the results suggest that the thickness of layers plays a crucial role in determining print time. Interestingly, the print angle, either alone or in combination with layer thickness, does not

significantly alter print times. The interaction plot illustrates that, generally, print time decreases as the layer thickness increases, regardless of the print angle. However, there is not a notable difference in print time among various print angles, though the shortest print times were observed at a 90° print angle.

In the case of print angle and infill density (Table 14), the analysis revealed that infill density significantly influences print time, while print angle and its interaction with infill density do not. According to the interaction plot for these variables, print time tends to decrease as infill density becomes lower, across all print angles.

Lastly, the analysis of layer thickness and infill density together (Table 15) found that both factors, along with their interaction, significantly affect print time. The interaction plot demonstrates that print time markedly decreases when infill density is lowered, across various layer thicknesses.

In summary, this analysis indicates that while certain printing parameters individually and in combination can significantly affect printing duration, others do not. Specifically, layer thickness and infill density are crucial factors that influence print time, whereas print angle plays a lesser role in this context.

**Table 13** Two-way ANOVA; print time (min) vs print angle (deg)-layer thickness (mm) interaction

Source	DF	SS	MS	F	P
Print Angle (deg)	6	1723	287.2	5.61	0.0
Layer Thickness (mm)	2	178158	89078.8	1740.59	0.0
Interaction	12	297	24.7	0.48	0.924
Error	294	15046	51.2		
Total	314	195224			

$S = 7.154$ ,  $R^2 = 92.29\%$ , and  $R^2$  (adj) = 91.77%

**Table 14** Two-way ANOVA: print time (min) vs print angle (deg)-infill density (%) interaction

Source	DF	SS	MS	F	P
Print angle (Deg)	6	1723	287.20	0.47	0.834
Infill density (%)	2	11442	5720.95	9.28	0.0
Interaction	12	749	62.43	0.10	1.0
Error	294	181309	616.70		
Total	314	195224			

$S = 24.83$ ,  $R^2 = 7.13\%$ , and  $R^2(\text{adj}) = 0.81\%$

**Table 15** Two-way ANOVA: print time (min) vs layer thickness (mm)-infill density (%) Interaction

Source	DF	SS	MS	F	P
Layer thickness (mm)	2	178158	89078.8	8158.84	0.0
Infill density (%)	2	11442	5721.0	523.99	0.0
Interaction	4	2283	570.8	52.28	0.0
Error	306	3341	10.9		
Total	314	195224			

$S = 3.304$ ,  $R^2 = 98.29\%$ , and  $R^2(\text{adj}) = 98.24\%$

**Fig. 9** Interaction plot for print time (min)

Effect of change in parameters on built time in correlation to tensile strength was evaluated by calculating tensile strength (MPa) per unit build-time (mins), as presented in Table 16. It should be noted that these values do not reflect any numerical entity. They are only calculated to find out the feasibility of printing a specimen at a specific set of parameters for a particular value of tensile strength in terms of time required to print that specimen. They can be used to decide if a trade-off is possible between tensile strength for built-time or vice-versa. A graphical comparison of tensile strength (MPa) to build-time (min) for all values of layer thickness at different level of infill densities and at different print angles is also shown in Fig. 10. The maximum value for tensile strength per unit time is found to 1.28 MPa/min and is observed for 90° raster angle at 0.3-mm layer thickness with 100% infill density.

**Table 16** Average tensile strength per unit build-time (MPa/min) for all specimens

		Average tensile strength to build-time (MPa/min)								
		Infill density 100%			Infill density 75%			Infill density 50%		
		Layer thickness (MM)			Layer thickness (MM)			Layer thickness (MM)		
		0.1	0.2	0.3	0.1	0.2	0.3	0.1	0.2	0.3
Print angle (DEG)	0	0.31	0.57	0.72	0.17	0.30	0.39	0.12	0.21	0.31
	15	0.31	0.57	0.72	0.18	0.32	0.40	0.12	0.21	0.31
	30	0.34	0.61	0.78	0.19	0.33	0.44	0.13	0.24	0.34
	45	0.38	0.68	0.89	0.22	0.37	0.49	0.16	0.26	0.38
	60	0.45	0.82	1.08	0.25	0.44	0.57	0.16	0.28	0.45
	75	0.47	0.88	1.14	0.29	0.54	0.70	0.21	0.38	0.47
	90	0.54	1.01	1.28	0.49	0.91	1.18	0.49	0.88	0.54

**Fig. 10** Tensile strength (MPa) per unit built-time (min), at different values of infill densities, layer thickness, and raster angles

### **3.3. Analysis for density**

Masses were recorded for all printed specimens to determine the actual density of each part. The cross-sectional area of each sample was measured using CAD software, and this value was then multiplied by the thickness of each sample to obtain its volume. The measured mass of each sample was subsequently divided by its volume to calculate its density. The findings from these calculations are presented in Table 17 for reference.

**Table 17** Measure density (gm/cm<sup>3</sup>)

		Measure densities (gm/cm <sup>3</sup> )								
		Infill density 100%			Infill density 75%			Infill density 50%		
		Layer thickness (MM)			Layer thickness (MM)			Layer thickness (MM)		
		0.1	0.2	0.3	0.1	0.2	0.3	0.1	0.2	0.3
Print angle (DEG)	0	1.102	1.047	1.081	0.938	0.913	0.903	0.791	0.757	0.727
	15	1.122	1.054	1.077	0.940	0.914	0.904	0.788	0.756	0.728
	30	1.101	1.048	1.077	0.932	0.916	0.899	0.781	0.758	0.724
	45	1.101	1.060	1.066	0.931	0.907	0.895	0.779	0.749	0.718
	60	1.108	1.056	1.061	0.921	0.908	0.900	0.786	0.761	0.725
	75	1.105	1.036	1.052	0.924	0.911	0.903	0.787	0.757	0.726
	90	1.094	1.057	1.041	0.924	0.906	0.893	0.777	0.747	0.711

The data shown in the Table 17 represents the average density calculated for each specimen. This calculated density value is then divided by the density of the PLA filament, which is typically 1.23 gm/cm<sup>3</sup>. The resulting values are expressed as percentages in Table 18. This calculation offers insights into the proportion of material contained within each specimen, providing insights into the relative density of the printed specimens compared to the density of the filament material used for printing.

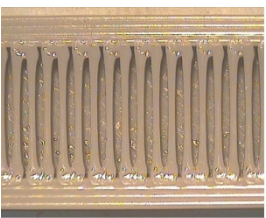
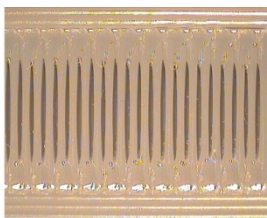
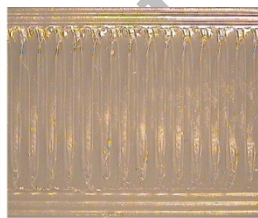
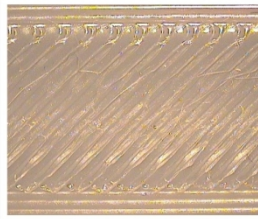
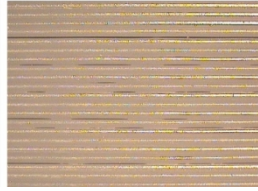
**Table 18** Density measured through weight expressed as (%) of the density of the filament material.

		Measure density (%age)								
		Infill density 100%			Infill density 75%			Infill density 50%		
		Layer thickness (MM)			Layer thickness (MM)			Layer thickness (MM)		
		0.1	0.2	0.3	0.1	0.2	0.3	0.1	0.2	0.3
Print angle (DEG)	0	89.6%	85.2%	87.9%	76.3%	74.2%	73.4%	64.3%	61.5%	59.1%
	15	91.2%	85.7%	87.5%	76.4%	74.3%	73.5%	64.1%	61.4%	59.2%
	30	89.5%	85.2%	87.5%	75.7%	74.5%	73.1%	63.5%	61.6%	58.9%
	45	89.5%	86.2%	86.7%	75.7%	73.8%	72.7%	63.3%	60.9%	58.4%
	60	90.1%	85.8%	86.3%	74.9%	73.9%	73.2%	63.9%	61.9%	59.0%
	75	89.9%	84.2%	85.5%	75.1%	74.0%	73.4%	64.0%	61.5%	59.1%
	90	88.9%	85.9%	84.6%	75.1%	73.7%	72.6%	63.2%	60.8%	57.8%

Table 19 presents a visual comparative study of the gaps between raster lines at three distinct printing angles across varying infill densities. The study examines three levels of infill density: 50%, 75%, and 100%, alongside three corresponding print angles: 0°, 45°, and 90°, respectively oriented in reference to the force direction (where 90° is along the direction of the applied force). These images shed light on how the spacing between raster lines varies under different infill densities and printing angles, providing valuable insights into their impact on the structural integrity and mechanical properties of the printed components. As observed, even though there are gaps between the raster lines at a 90° angle, these lines will consistently align with the direction of the applied force and carry the load. In contrast, for angles below 90°, the spacing between raster lines leads to a decrease in the number of load-bearing nodes, significantly weakening the specimen.

Accepted manuscript

**Table 19** Gaps comparison between the rasters at different infill densities for 0°, 45°, and 90° raster angles. (Images captured through stereo-microscope at 5x zoom)

		Infill density		
		50%	75%	100%
Print Angle (Deg)	0°			
	45°			
	90°			

### 3.4. Analysis for top-bottom layers and perimeter shells

To investigate the load-bearing capacity of the top and bottom layers along with the perimeter shells of 3D-printed samples, experiments were conducted using a  $0^\circ$  print angle and layer thicknesses of 0.1 mm, 0.2 mm, and 0.3 mm, combined with infill densities of 10%, 20%, and 40%. All other print parameters are kept constant as per Table 4. The choice of a  $0^\circ$  print angle ensures that the infill rasters do not bear any load themselves but merely support the top layer to prevent it from caving in. Using three levels of low infill density (10%, 20%, and 40%) aims to eliminate any strength contribution from the specimen's core, also highlighting the significant drop in tensile strength noted at 75% and 50% infill densities when printed at lower angles. Varying the layer thickness helps to assess its influence on the structural integrity of the top-bottom layers and perimeter shells. Figure 11 displays the cross-section of the printed samples, showing how the internal rasters primarily serve as supports for the external structure, preventing it from collapsing inwards. The spacing between these internal rasters is determined by the varying levels of infill density chosen for the prints.

**Fig. 11** Cross-section of tensile test specimens for top-bottom layer and perimeter shells **a** at 50% infill density, **b** at 20% infill density, and **c** at 10% infill density.

To ensure the reliability of the results, five replicates of each combination of conditions were printed and subjected to testing. The average tensile strength values for these specimens are documented in Table 20. This table reveals that tensile strength decreases with changes in both infill density and layer thickness. Specifically, the reduction in tensile strength associated with changes in layer thickness mirrors the reduction seen at 100% infill density and a  $0^\circ$  print angle. Likewise, the decline in tensile strength due to changes in infill density follows a consistent pattern with the reductions observed at 75% and 50% infill densities.

**Table 20** Average values for combined tensile strength of top-bottom layers and number of perimeter shells.

Tensile strength for top-bottom layers & perimeter shells (MPa)			
Print angle 0°			
Infill density (%)	Layer thickness (MM)		
	0.1	0.2	0.3
10	7.85	7.32	6.95
20	7.97	7.43	7.03
40	9.05	8.42	7.87

## 4. Discussion

The tensile testing results depicted in Fig. 4 clearly illustrate an improvement in the part's strength when the raster angle was changed from 0 to 90° (i.e., when the rasters shifted from “perpendicular to the direction of applied tension” to “in-line with the direction of applied tension”). Similar findings were observed in previous studies [18, 21, 25], where strength increased with the rise in raster angle. This suggests that most of the load is carried by the raster itself rather than the inter-raster bonding. At 0° raster angle, the inter-raster bonding bears the overall load, resulting in least strength compared to components with greater raster angles. Conversely, in components with raster angles at 90°, all the load is borne by the rasters themselves, resulting in highest strength values. The analysis using ANOVA, as shown in Table 7, indicates that the print angle significantly affects the tensile strength of the material, accounting for 26.81% of the variation in tensile strength. This means that changes in the print angle can lead to notable differences in the material's tensile strength. Furthermore, according to the results from a two-way ANOVA analysis, the combined effect (interaction) of print angle and infill density on tensile strength is significant, suggesting that these two factors together influence tensile strength in a meaningful way. However, the combined effect of print angle and layer thickness on tensile strength does not show a significant impact, indicating that these two factors together do not notably affect the tensile strength of the material. Table 11 illustrates the diverse print times associated with different raster angles. However, it's noteworthy that the relationship between print time and print angle does not follow a linear progression or a smooth curve and is different for different value of print angle. Nonetheless, it can be inferred from Fig. 7 that the time required to print parts decreases with the increase in raster angle from 0 to 90°. Unlike its impact on tensile strength, the print angle does not significantly affect the printing time, according to ANOVA analysis results shown in Table 12. Additionally, when examining the combined effects of print angle with other factors through a two-way ANOVA analysis, it was found that both the interaction of print angle with layer thickness and the interaction of print angle with infill density do not play a significant role in determining the printing time. This means that changing the print angle, either alone or in combination with changes in layer thickness or infill density, does not have a noticeable impact on how long it takes to print an object.

Moreover, it can also be observed from Fig. 4 that at a constant density, larger layer thickness results in weaker parts. The maximum value of tensile strength (MPa) for each value of the raster angle was observed at a minimum layer thickness (i.e., 0.1 mm). These results correlate with the findings of other studies [17, 20, 24, 29]. The observed results can be explained by considering the effects of using a smaller layer thickness in Fused Deposition Modeling (FDM). When the layer thickness is reduced, the individual layers of material become thinner. This finer approach to layering has two primary consequences for the internal structure of the printed object. First, it leads to a decrease in both the size and the number of voids or gaps that are typically found between the rasters, which are the lines of material laid down by the printer. These voids can be detrimental to the structural integrity and strength of the printed part. With thinner layers, the material is able to more effectively fill in these gaps, reducing their prevalence. Secondly, a smaller layer thickness allows the material to be packed more densely within the geometry of the component. This denser packing of material contributes to a more uniform internal structure, enhancing the overall strength and stability of the printed object. Therefore, opting for a smaller layer thickness in FDM not only improves the surface quality of the print but also positively impacts its internal consistency and structural integrity (see Fig. 12). Although reducing layer thickness appears to enhance tensile strength, ANOVA analysis reveals that layer thickness is not identified as a significant factor in itself. Similarly, the interactions of layer thickness with print angle and with infill density also do not show significant effects, based on the results from two-way ANOVA analysis. This could be attributed to the observation that alterations in print angle or infill density result in more pronounced changes in tensile strength compared to the variations in tensile strength caused by changes in layer thickness.

**Fig. 12** Comparison of internal structure (fracture surface) with different layer thickness at 60x optical zoom. **a** 0.1-mm layer thickness. **b** 0.2-mm layer thickness. **c** 0.3-mm layer thickness.

However, it is worth noting that smaller layer heights also increase the total number of layers and thus the printing time. This trade-off between quality and printing efficiency is a key

consideration when choosing the optimal layer height for a specific print job. Therefore, the choice of layer height in FDM printing depends on balancing the required quality and detail resolution with the acceptable printing time and material usage for the project. Table 11 demonstrates that the build time for the same raster angle at a fixed infill density but higher layer thickness is less compared to that of lower layer thickness. Fig. 10 illustrates that the “tensile strength–build time” values for higher layer thickness are greater than those of lower layer thicknesses. This is due to the fact that while lower layer thickness can increase the tensile strength (MPa) of the specimen, it also increases the time required to build the part. Therefore, if built-time is a constraint, then higher layer thickness is suggested. The analysis of variance demonstrates that layer thickness significantly affects the duration of printing, accounting for a substantial 92.09% of the total variation in print time. Furthermore, the combined effect (interaction) of layer thickness with infill density is identified as a significant factor, impacting how long the printing process takes. However, the interaction between layer thickness and print angle does not show a significant influence on print time. This suggests that while the thickness of the layers largely dictates the overall printing duration, its interaction with the density of the fill inside the model significantly contributes to this effect, whereas the orientation or angle of printing, when considered alongside layer thickness, does not significantly alter the time it takes to print.

Furthermore, it can also be observed from Fig. 4 that the variations in infill density have a notable effect on the overall strength of a 3D-printed part. This is evident from the observation that the highest tensile strength is achieved when the infill density is at its maximum, which is 100%. Infill density refers to how much of the interior volume of the print is filled with material, as opposed to being hollow or partially hollow. At a 100% infill density, the material is packed comprehensively throughout the internal volume of the part’s geometry. This dense packing means that there is more material available to absorb and distribute the forces applied to the part, thereby enhancing its ability to withstand loads without failing. In essence, a higher infill density leads to a stronger and more robust part because the material structure inside is more continuous and less prone to weaknesses that can arise from gaps or voids. These findings align with prior researches [16, 17, 20, 24, 32, 33]. The ANOVA analysis indicates that infill density is the most critical factor affecting tensile strength, accounting for 73.14% of the variation in tensile strength. This means that the density of the material inside the print plays a key role in

determining how strong the finished part will be. Additionally, the two-way ANOVA analysis also reveals that the infill density combined with print angle has a significant impact on tensile strength. However, the interaction between layer thickness and infill density does not significantly affect tensile strength, implying that changes in the thickness of individual layers do not meaningfully alter the strength impact of infill density. When the infill density is low, the printing process requires less time. This efficiency is due to the reduced number of linear patterns, or rasters, needed to fill the internal space of the part at lower densities, which leads to shorter printing times. With less infill density, a smaller quantity of material is used, allowing the print head to cover more area in less time. Consequently, components are printed more quickly because the print head moves faster across the print area due to fewer material deposits. This makes low infill density a key factor in speeding up the printing process. The ANOVA analysis detailed in Table 12 shows that, after other factors, infill density ranks as the second most influential factor on print time, contributing 7.73% to the overall variance in how long printing takes. Further exploration through a two-way ANOVA indicates that the way infill density combines with print angle does not significantly affect print time. However, the interaction between infill density and layer thickness does have a significant impact. This means that while changing the print angle does not markedly alter the effect of infill density on print time, altering layer thickness in conjunction with infill density does significantly influence how long the printing process will take. It should be highlighted that reducing the density of a printed part leads to an increase in the volume of voids and gaps within its internal structure (see Fig. 13). Figure 13 highlights that the infill density of a specimen has a more substantial impact on its properties than the layer thickness does. By comparing Figures 12 and 13, it becomes evident that the voids and gaps resulting from increased layer thickness are significantly smaller than those created by reducing infill density. This comparison indicates that reducing the infill density affects the specimen's structure more dramatically than adjusting the thickness of each layer. The densities of all specimens were calculated by measuring their masses and dividing them by their volumes. These values, presented in Table 17, reflect a reduction in the actual densities of the parts due to increased voids and gaps within the infill. However, it is also observed that the drop in the measured density of the specimen is not proportional to the change or drop in the infill density. This discrepancy arises because the top and bottom layers and the perimeter shells are

printed at 100% density. The measured density as a percentage of the density of filament material is outlined in Table 18.

**Fig. 13** Comparison of internal structure (fracture surface) with different layer thickness at 60x optical zoom. **a** 0.1-mm layer thickness and 75% infill density. **b** 0.2-mm layer thickness and 75% infill density. **c** 0.3-mm layer thickness and 75% infill density. **d** 0.1-mm layer thickness and 50% infill density. **e** 0.2-mm layer thickness and 50% infill density. **f** 0.3-mm layer thickness and 50% infill density.

This study revealed a distinctive pattern in how the tensile strength of a 3D-printed part responds to changes in infill density at various raster angles. Notably, for specimens printed with a raster angle of 90°, there is a proportional relationship between tensile strength and infill density. This means that as the infill density decreases, the tensile strength of the part also diminishes in a consistent manner. As previously mentioned, in 3D-printed parts, the rasters bear most of the load, while the bonding between the rasters supports a smaller portion of the load. In specimens with a raster angle of 90°, a reduction in infill density leads to a proportional decrease in the number of rasters. In these specimens, the rasters themselves are primarily responsible for carrying the load, with minimal reliance on the bonding between rasters. Consequently, the tensile strength decreases proportionally with the reduction in the number of rasters. Specimens with raster angles below 90° display a distinctively different response when infill density decreases, leading to a notable decline in tensile strength that suggests a nonlinear correlation. Table 19 features images that highlight how reduced infill densities increase the space between raster lines, reducing the number of rasters and consequently, the material available for load support and distribution. This shortage of material and greater raster spacing weaken the part's structural integrity and accelerate crack propagation. Importantly, at angles below 90 degrees, the strength of the part relies more heavily on the bonding between rasters for load distribution. With a decrease in infill density, the reduction in rasters and the widening of gaps between them undermine this crucial bonding, diminishing the part's ability to distribute loads effectively. This

leads to an increased likelihood of part failure under reduced loads, particularly at raster angles below  $90^\circ$ , where tensile strength significantly decreases due to these changes. This observation also highlights that for the specimen with low infill density and print angles below  $90^\circ$ , substantial portion of the tensile strength in a printed specimen is provided by the top and bottom layers, along with the perimeter shells since there is not enough contribution by the inner core of the specimen subjected to the gap and voids produced as a result for decreasing infill density. Moreover, it can be observed through the values of tensile strength presented in Table 20 that almost one-fourth of the total strength is bore by the top and bottom layers and perimeter shells of the specimen.

## 5. Conclusion

Layer thickness, raster angle, and infill density were varied as process parameters to print PLA specimens on the FDM printer. Tensile tests were conducted following ISO-527-2 standards to assess the influence of these parameters. The values obtained from the tensile tests and the build time required for each sample were recorded to study their effects on both aspects and to develop a trade-off for tensile strength, especially when printing time is a constraint.

The findings of this research revealed that the tensile strength of the printed specimens increases as the raster angle changes from  $0$  to  $90^\circ$  (where  $0^\circ$  indicates rasters perpendicular to the applied load and  $90^\circ$  indicates rasters parallel to the applied load). This indicates that the rasters themselves bear more load than the inter-raster bonding. Meanwhile, the printing time remained consistent across all values of raster angle, rendering it a negligible factor in influencing print time. Hence, for improved tensile strength higher values of raster angle is suggested.

Additionally, for all raster angle values, tensile strength increases and print time decrease with the increase in layer height. Moreover, the ANOVA analysis revealed that layer thickness is insignificant factor for tensile strength but markedly significant factor for print time. Therefore, if built-time is a constraint, then higher layer thickness is suggested.

Similarly, tensile strength of the specimen and time require to print it, both increases with higher infill density. The result is also supported by ANOVA analysis where infill density is significant factor for both responses (tensile strength and print time). However, as per the findings of this

research, it is not recommended to employ low infill densities with print angles below  $90^\circ$ , since the combine effect of both results in a drastic drop of tensile strength.

### **Acknowledgements**

We would like to express our sincere gratitude to NED University of Engineering and Technology for providing the essential funding that made this research possible and to the Pakistan Space and Upper Atmosphere Research Commission (SUPARCO) for their invaluable support in providing the facility to conduct the necessary testing for this research.

### **Author contribution**

All authors contributed to the study conception and design. Material preparation and data collection were performed by Mr. Asif Hasan and Dr. Muhammad Fahad. Analysis was performed by Mr. Asif Hasan under the supervision of Dr. Maqsood Ahmed Khan. The first draft of the manuscript was written by Mr. Asif Hasan, and all authors commented on previous versions of the manuscript. All authors read and approved the final manuscript.

### **Funding**

This work was funded by NED University of Engineering & Technology, Karachi, Pakistan. Author Mr. Asif Hasan has received research grant from NED University.

### **Declarations**

### **Competing interests**

The authors declare no competing interests.

## References

- [1] “Additive manufacturing - General principles - Fundamentals and vocabulary:,” BSI British Standards. doi: 10.3403/30448424.
- [2] I. Gibson, D. Rosen, and B. Stucker, *Additive Manufacturing technologies: 3D printing, rapid prototyping, and direct digital manufacturing*. New York, NY: Springer New York, 2015. doi: 10.1007/978-1-4939-2113-3.
- [3] S. H. Masood, “Advances in fused deposition modeling,” in *Comprehensive Materials Processing*, Elsevier, 2014, pp. 69–91. doi: 10.1016/B978-0-08-096532-1.01002-5.
- [4] M. Fahad, M. Mujeeb, and M. A. Khan, “Effect of process parameters on the compressive and impact strength of 3D printed parts,” *Iran J Sci Technol Trans Mech Eng*, vol. 47, no. 1, pp. 257–265, Mar. 2023, doi: 10.1007/s40997-022-00514-z.
- [5] A. K. Kamrani and E. A. Nasr, *Engineering design and rapid prototyping*. Boston, MA: Springer US, 2010. doi: 10.1007/978-0-387-95863-7.
- [6] M. Savastano, C. Amendola, F. D’Ascenzo, and E. Massaroni, “3-D printing in the spare parts supply chain: an explorative study in the automotive industry,” in *Digitally Supported Innovation*, vol. 18, L. Caporarello, F. Cesaroni, R. Giesecke, and M. Missikoff, Eds., Springer International Publishing, 2016, pp. 153–170.
- [7] O. Ivanova, C. Williams, and T. Campbell, “Additive manufacturing (AM) and nanotechnology: promises and challenges,” *Rapid Prototyping Journal*, vol. 19, no. 5, pp. 353–364, Jul. 2013, doi: 10.1108/RPJ-12-2011-0127.
- [8] A. K. Sood, R. K. Ohdar, and S. S. Mahapatra, “Parametric appraisal of mechanical property of fused deposition modelling processed parts,” *Materials & Design*, vol. 31, no. 1, pp. 287–295, Jan. 2010, doi: 10.1016/j.matdes.2009.06.016.
- [9] D. Popescu, A. Zapciu, C. Amza, F. Baci, and R. Marinescu, “FDM process parameters influence over the mechanical properties of polymer specimens: a review,” *Polymer Testing*, vol. 69, pp. 157–166, Aug. 2018, doi: 10.1016/j.polymertesting.2018.05.020.

- [10] M. Montero, S. Roundy, D. Odell, S.-H. Ahn, and P. K. Wright, "Material characterization of fused deposition modeling (FDM) ABS by designed experiments," 2001.
- [11] H. Liu and J. Zhang, "Research progress in toughening modification of poly(lactic acid)," *J. Polym. Sci. B Polym. Phys.*, vol. 49, no. 15, pp. 1051–1083, Aug. 2011, doi: 10.1002/polb.22283.
- [12] R. Hagen, "Polylactic acid," in *Polymer science: a comprehensive reference*, Elsevier, 2012, pp. 231–236. doi: 10.1016/B978-0-444-53349-4.00269-7.
- [13] S. Saeidlou, M. A. Huneault, H. Li, and C. B. Park, "Poly(lactic acid) crystallization," *Progress in Polymer Science*, vol. 37, no. 12, pp. 1657–1677, Dec. 2012, doi: 10.1016/j.progpolymsci.2012.07.005.
- [14] T. Casalini, F. Rossi, A. Castrovinci, and G. Perale, "A perspective on polylactic acid-based polymers use for nanoparticles synthesis and applications," *Front. Bioeng. Biotechnol.*, vol. 7, p. 259, Oct. 2019, doi: 10.3389/fbioe.2019.00259.
- [15] B. M. Tymrak, M. Kreiger, and J. M. Pearce, "Mechanical properties of components fabricated with open-source 3-D printers under realistic environmental conditions," *Materials & Design*, vol. 58, pp. 242–246, Jun. 2014, doi: 10.1016/j.matdes.2014.02.038.
- [16] C. A. Griffiths, J. Howarth, G. de-Almeida Rowbotham, and A. Rees, "Effect of build parameters on processing efficiency and material performance in fused deposition modelling," *Procedia CIRP*, vol. 49, pp. 28–32, 2016, doi: 10.1016/j.procir.2015.07.024.
- [17] H. Li, T. Wang, and Z. Yu, "The quantitative research of interaction between key parameters and the effects on mechanical property in FDM," *Advances in Materials Science and Engineering*, vol. 2017, pp. 1–15, 2017, doi: 10.1155/2017/9152954.
- [18] S. R. Rajpurohit and H. K. Dave, "Effect of raster angle on tensile properties of PLA part fabricated using fused deposition modeling process," 2017.
- [19] H. Li, T. Wang, J. Sun, and Z. Yu, "The effect of process parameters in fused deposition modelling on bonding degree and mechanical properties," *RPJ*, vol. 24, no. 1, pp. 80–92, Jan. 2018, doi: 10.1108/RPJ-06-2016-0090.

- [20] K. Li, L. Liu, J. Wu, M. Li, and S. Yong, "Study on the mechanical performance optimization of FDM built parts," in *Applied Sciences in Graphic Communication and Packaging*, vol. 477, P. Zhao, Y. Ouyang, M. Xu, L. Yang, and Y. Ren, Eds., in Lecture Notes in Electrical Engineering, vol. 477. , Singapore: Springer Singapore, 2018, pp. 563–569. doi: 10.1007/978-981-10-7629-9\_69.
- [21] S. R. Rajpurohit and H. K. Dave, "Prediction and optimization of tensile strength in FDM based 3D printing using ANFIS," in *Optimization of Manufacturing Processes*, K. Gupta and M. K. Gupta, Eds., in Springer Series in Advanced Manufacturing. , Cham: Springer International Publishing, 2020, pp. 111–128. doi: 10.1007/978-3-030-19638-7\_5.
- [22] J. Giri, A. Chiwande, Y. Gupta, C. Mahatme, and P. Giri, "Effect of process parameters on mechanical properties of 3d printed samples using FDM process," *Materials Today: Proceedings*, vol. 47, pp. 5856–5861, 2021, doi: 10.1016/j.matpr.2021.04.283.
- [23] M. Ouhsti, B. El Haddadi, and S. Belhouideg, "Effect of printing parameters on the mechanical properties of parts fabricated with open-source 3D printers in PLA by fused deposition modeling," *Mechanics and Mechanical Engineering*, vol. 22, no. 4, pp. 895–908, Dec. 2018, doi: 10.2478/mme-2018-0070.
- [24] A. Rodríguez-Panes, J. Claver, and A. Camacho, "The influence of manufacturing parameters on the mechanical behaviour of PLA and ABS pieces manufactured by FDM: a comparative analysis," *Materials*, vol. 11, no. 8, p. 1333, Aug. 2018, doi: 10.3390/ma11081333.
- [25] A. Lanzotti, M. Grasso, G. Staiano, and M. Martorelli, "The impact of process parameters on mechanical properties of parts fabricated in PLA with an open-source 3-D printer," *Rapid Prototyping Journal*, vol. 21, no. 5, pp. 604–617, Aug. 2015, doi: 10.1108/RPJ-09-2014-0135.
- [26] Y. Song, Y. Li, W. Song, K. Yee, K.-Y. Lee, and V. L. Tagarielli, "Measurements of the mechanical response of unidirectional 3D-printed PLA," *Materials & Design*, vol. 123, pp. 154–164, Jun. 2017, doi: 10.1016/j.matdes.2017.03.051.

- [27] Z. Yu *et al.*, “Study on effects of FDM 3D printing parameters on mechanical properties of polylactic acid,” *IOP Conf. Ser.: Mater. Sci. Eng.*, vol. 688, no. 3, p. 033026, Nov. 2019, doi: 10.1088/1757-899X/688/3/033026.
- [28] A. Tsouknidas, M. Pantazopoulos, I. Katsoulis, D. Fasnakis, S. Maropoulos, and N. Michailidis, “Impact absorption capacity of 3D-printed components fabricated by fused deposition modelling,” *Materials & Design*, vol. 102, pp. 41–44, Jul. 2016, doi: 10.1016/j.matdes.2016.03.154.
- [29] X. Liu, M. Zhang, S. Li, L. Si, J. Peng, and Y. Hu, “Mechanical property parametric appraisal of fused deposition modeling parts based on the gray Taguchi method,” *Int J Adv Manuf Technol*, vol. 89, no. 5–8, pp. 2387–2397, Mar. 2017, doi: 10.1007/s00170-016-9263-3.
- [30] O. Lužanin, D. Movrin, and M. Plan, “Effect of layer thickness, deposition angle, and infill on maximum flexural force in fdm-built specimens,” *Journal for Technology of Plasticity*, vol. 39, no. 1, 2014.
- [31] J. M. Chacón, M. A. Caminero, E. García-Plaza, and P. J. Núñez, “Additive manufacturing of PLA structures using fused deposition modelling: effect of process parameters on mechanical properties and their optimal selection,” *Materials & Design*, vol. 124, pp. 143–157, Jun. 2017, doi: 10.1016/j.matdes.2017.03.065.
- [32] J. Torres, M. Cole, A. Owji, Z. DeMastry, and A. P. Gordon, “An approach for mechanical property optimization of fused deposition modeling with polylactic acid via design of experiments,” *RPJ*, vol. 22, no. 2, pp. 387–404, Mar. 2016, doi: 10.1108/RPJ-07-2014-0083.
- [33] A. Alafaghani, A. Qattawi, B. Alrawi, and A. Guzman, “Experimental optimization of fused deposition modelling processing parameters: a design-for-manufacturing approach,” *Procedia Manufacturing*, vol. 10, pp. 791–803, 2017, doi: 10.1016/j.promfg.2017.07.079.
- [34] Y. Tao, P. Li, and L. Pan, “Improving Tensile Properties of Polylactic Acid Parts by Adjusting Printing Parameters of Open Source 3D Printers,” *ms*, vol. 26, no. 1, pp. 83–87, Nov. 2019, doi: 10.5755/j01.ms.26.1.20952.

- [35] Ei Cho and Thanh Tran, "Investigation on influence of infill pattern and layer thickness on mechanical strength of PLA material in 3D printing technology," *JESR*, vol. 3, no. 2, pp. 27–37, Apr. 2019, doi: 10.26666/rmp.jesr.2019.2.5.
- [36] L. Le, M. A. Rabsatt, H. Eisazadeh, and M. Torabizadeh, "Reducing print time while minimizing loss in mechanical properties in consumer FDM parts," *International Journal of Lightweight Materials and Manufacture*, vol. 5, no. 2, pp. 197–212, Jun. 2022, doi: 10.1016/j.ijlmm.2022.01.003.
- [37] R. D. Bintara, D. Z. Lubis, and Y. R. Aji Pradana, "The effect of layer height on the surface roughness in 3D printed polylactic acid (PLA) using FDM 3D printing," *IOP Conf. Ser.: Mater. Sci. Eng.*, vol. 1034, no. 1, p. 012096, Feb. 2021, doi: 10.1088/1757-899X/1034/1/012096.
- [38] S. Maurya, B. Malik, P. Sharma, A. Singh, and R. Chalisgaonkar, "Investigation of different parameters of cube printed using PLA by FDM 3D printer," *Materials Today: Proceedings*, vol. 64, pp. 1217–1222, 2022, doi: 10.1016/j.matpr.2022.03.700.
- [39] *Plastics. Determination of tensile properties Test conditions for moulding and extrusion plastics*, Revision Underway. 2012.